Annu. Rev. Fluid Mech. 2005. 37:129–49
doi: 10.1146/annurev.fluid.36.050802.122132

FLUID MECHANICS AND RHEOLOGY OF DENSE SUSPENSIONS

Jonathan J. Stickel and Robert L. Powell
Department of Chemical Engineering and Materials Science, University of California, Davis, California 95616; email: jjstickel@ucdavis.edu, rlpowell@ucdavis.edu

Key Words concentrated, microstructure, non-Newtonian

■ **Abstract** We review the fluid mechanics and rheology of dense suspensions, emphasizing investigations of microstructure and total stress. "Dense" or "highly concentrated" suspensions are those in which the average particle separation distance is less than the particle radius. For these suspensions, multiple-body interactions as well as two-body lubrication play a significant role and the rheology is non-Newtonian. We include investigations of multimodal suspensions, but not those of suspensions with dominant nonhydrodynamic interactions. We consider results from both physical experiments and computer simulations and explore scaling theories and the development of constitutive equations.

1. INTRODUCTION

Suspensions of solid particles in a viscous liquid are ubiquitous, with examples in biological systems (blood), home products (paint), and industrial processing (waste slurries). Suspensions are a class of complex fluids and can be further differentiated according to the physical and chemical nature of the suspended particles and suspending fluid. We consider here neutrally buoyant, chemically stable (nonaggregating) hard particles in a Newtonian fluid. The particles are considered spherical, or at least have a geometric aspect ratio close to one, thus excluding suspensions of fibers and rods. We are particularly interested in dense suspensions. "Dense" or "highly concentrated" can be defined in a few ways, including: (*a*) the average separation distance between the particles is equal to or smaller than the particle size, (*b*) multiple-body interactions as well as two-body lubrication contribute significantly to the rheology of the suspension, and (*c*) the rheology is non-Newtonian. We loosely adhere to all of these definitions.

At the length scale of the particles, the mechanics of these systems are governed by the Navier-Stokes equations. Solutions could theoretically be found for each particle, but due to the multibody interactions the mathematics becomes complicated with even just a few. At length scales greater than ∼100-particle radii, it is reasonable to consider the suspension as a continuum. This is appropriate for most applications because many suspended particles are less than a few micrometers in diameter.

The mechanics of dilute and semidilute suspensions are well understood, primarily due to the work of Einstein (1956), Batchelor (1970, 1977), and Batchelor & Green (1972). However, constitutive equations relating stress to rate of strain for concentrated suspensions are not generally known, and hence their rheology is still a subject of much investigation despite a considerable amount of work over the past century. Experimentation has revealed the unique behavior of fluid suspensions including shear-thinning and thixotropy, shear-thickening and rheopexy, and yield stresses (Sato 1995). In particular, there have been numerous studies of suspension viscosity as a function of particle concentration and composition. So many theoretical and empirical models have resulted that it is difficult to find a unifying theme. In this review we emphasize that microstructure is the key to understanding the fluid mechanics and rheology of concentrated suspensions. Microstructure (often termed simply structure) refers to the relative position and orientation of physical entities in a material. Microstructure not only provides a means to explain viscosity relations for suspensions, but it also is vital to the understanding of normal-stress differences and the development of constitutive equations.

Computer simulations have made a significant contribution to our understanding of suspension mechanics and rheology. Barnes et al. (1987) gave a comprehensive review, but simulation methods have progressed considerably since then. The most widely used method for simulating suspension flow at low-particle Reynolds number has been Stokesian dynamics (Brady & Bossis 1988, Sierou & Brady 2001), in which the linear equations describing Stokes flow are simultaneously solved at discrete time steps for all the particles in the simulation. Other notable simulation techniques are dissipative particle dynamics (Boek et al. 1997, Hoogerbrugge & Koelman 1992), the lattice Boltzmann method (Chen & Doolen 1998, Hill et al. 2001), and the Lagrange multiplier fictitious domain method (Glowinski et al. 1999, Singh et al. 2003). We do not explore the details of simulation development and their use; the references cited above are satisfactory. Instead, we use the results from computer simulations equally with those from physical experiments to explore the unique behavior of "dense" fluid suspensions.

We start in section 2 with a brief look at the appropriate dimensional analysis for suspension rheology. This provides a guide to the variables of interest. Section 3 gives an overview of suspension viscosity studies and a few mathematical relations that result. In section 4 we discuss the mechanics of concentrated suspensions, and in section 5 we discuss shear-induced particle diffusion, a special phenomenon of concentrated suspension flow. Section 6 provides some summary comments and points the way for future work.

2. DIMENSIONAL ANALYSIS

We begin with the general form of the conservation of linear momentum:

$$\rho \frac{\mathrm{D}\mathbf{v}}{\mathrm{D}t} = \rho \mathbf{g} + \boldsymbol{\nabla} \cdot \boldsymbol{\Pi}, \tag{1}$$

where $\mathbf{v}$ is the velocity vector, $\mathbf{\Pi}$ the total stress tensor, ρ the density, and $\frac{\mathrm{D}}{\mathrm{D}t}$ the material derivative. It is often convenient to define a deviatoric stress as $\tau := \mathbf{\Pi} + p\mathbf{I}$, where p is the pressure and $\mathbf{I}$ is the unit tensor. For incompressible materials, the deviatoric stress is the constitutive stress. It is often related to the rate of deformation tensor, $\dot{\gamma} := \frac{1}{2}(\boldsymbol{\nabla}\mathbf{v} + (\boldsymbol{\nabla}\mathbf{v})^T)$, as

$$\boldsymbol{\tau} = \boldsymbol{\tau}(\dot{\gamma}). \tag{2}$$

We return to these equations and consider them more fully in sections 4 and 5.

By far, the most widely used flow to probe the rheology and structure of suspensions is shear flow. For a dimensional analysis of shear flow the scalar shear stress, $\tau = \frac{1}{\sqrt{2}}|\boldsymbol{\tau}|$, and the rate of deformation, $\dot{\gamma} = \sqrt{2}|\dot{\gamma}|$, are used ($|\mathbf{A}| := \sqrt{\mathbf{A} : \mathbf{A}}$), and the viscosity is defined as $\eta := \frac{\tau}{\dot{\gamma}}$. The dimensional analysis given here follows that of Krieger (1963, 1972) and more recently Jomha et al. (1991).

We consider the viscosity of the suspension as a general function of several system parameters:

$$\eta = f(a, \rho_p, n, \eta_0, \rho_0, kT, \dot{\gamma} \text{ or } \tau, t), \tag{3}$$

where we have particle properties: radius a, density ρ_p, and number concentration n; suspending medium properties: viscosity η_0 and density ρ_0; thermal energy kT; the shear variable: shear rate $\dot{\gamma}$ or shear stress τ; and time t. For suspensions with more than one particle size, the average radius should be used for a, and one or more additional terms would be necessary to represent the particle-size distribution. All of the terms in Equation 3 can be expressed in units of mass, length, and time. By forming dimensionless groups this equation can be reduced to $9-3=6$ variables:

$$\eta_r = f(\phi, \rho_r, \mathrm{Pe}_{\dot{\gamma}}, \mathrm{Re}_{\dot{\gamma}}, t_r), \tag{4}$$

where

$$\eta_r = \frac{\eta}{\eta_0}, \qquad \phi = \frac{4\pi}{3} n a^3,$$

$$\rho_r = \frac{\rho_p}{\rho_0}, \qquad \mathrm{Pe}_{\dot{\gamma}} = \frac{6\pi\eta_0 a^3 \dot{\gamma}}{kT},$$

$$\mathrm{Re}_{\dot{\gamma}} = \frac{\rho_0 a^2 \dot{\gamma}}{\eta_0}, \quad \text{and} \quad t_r = \frac{tkT}{\eta_0 a^3}.$$

We chose $\dot{\gamma}$ rather than τ for the shear variable. Equation 4 may be further simplified for several important cases. For neutrally buoyant systems at steady-state, ρ_r and t_r may be neglected:

$$\eta_r = f(\phi, \mathrm{Pe}_{\dot{\gamma}}, \mathrm{Re}_{\dot{\gamma}}). \tag{5}$$

Krieger assumed for his systems ($a \sim 1\,\mu$m) that the Reynolds number was vanishingly small ($\mathrm{Re}_{\dot{\gamma}} \to 0$) and proposed a semiempirical equation for $\eta_r = f(\phi, \mathrm{Pe}_{\dot{\gamma}})$. Alternatively, we may consider non-Brownian systems for which the

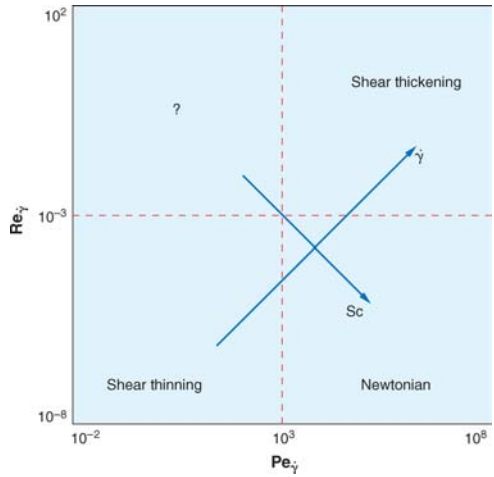

Figure 1 "Phase diagram" for suspension rheology, based solely on a dimensional analysis.

Peclet number is very large ($\mathrm{Pe}_{\dot{\gamma}} \to \infty$) and $\eta_r = f(\phi, \mathrm{Re}_{\dot{\gamma}})$. If we assume that both $\mathrm{Pe}_{\dot{\gamma}}$ and $\mathrm{Re}_{\dot{\gamma}}$ can be neglected, as have some authors (Chang & Powell 2002, Probstein et al. 1994, Shapiro & Probstein 1992), then

$$\eta_r = f(\phi) \tag{6}$$

only. This implies that the viscosity is a unique value at every concentration and hence the suspensions are Newtonian. Both $\mathrm{Pe}_{\dot{\gamma}}$ and $\mathrm{Re}_{\dot{\gamma}}$ can be neglected, i.e., $\mathrm{Re}_{\dot{\gamma}} \lesssim 10^{-3}$ and $\mathrm{Pe}_{\dot{\gamma}} \gtrsim 10^3$, for only a relatively narrow window of shear rates, given values of a, η_0, and ρ_0. The size of this "window" scales according to the Schmidt number, $\mathrm{Sc} = \frac{\mathrm{Pe}_{\dot{\gamma}}}{\mathrm{Re}_{\dot{\gamma}}} = \frac{6\pi\eta^2 a}{\rho_0 kT}$. A suspension may be expected to behave as a Newtonian fluid for greater ranges of shear rate as particle size and fluid viscosity increase, such that $\mathrm{Sc} \gg 1$ (Figure 1). We discuss this more in section 3.

3. SUSPENSION VISCOSITY

There are abundant viscosity versus shear rate (or shear stress) data in the literature for fluid-particle suspensions (e.g., Figure 2). Non-Newtonian behavior is generally observed for solids concentrations exceeding 0.4 by volume. Observing data like these, many authors have found it convenient to assume that concentrated suspensions are generally shear-thinning with Newtonian limiting behavior at both low and high shear rates. This is not necessarily the case.

The reported high shear rate limit is a Newtonian plateau before the onset of shear-thickening as the shear rate increases (Hoffman 1972, Jomha et al. 1991,

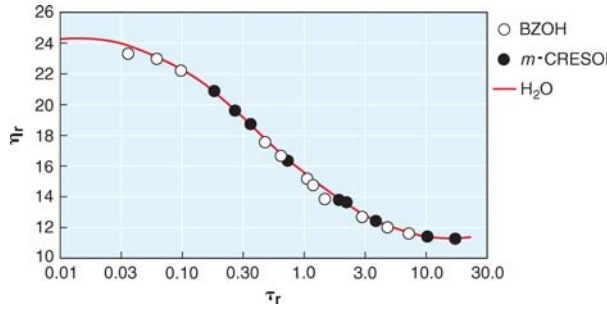

Figure 2 Reduced viscosity versus reduced stress for 1 μm spherical particles in the fluids indicated. Reprinted from Krieger (1972) with permission from Elsevier ©1972.

Metzner & Whitlock 1958, So et al. 2001). Hoffman's (1972) results clearly illustrate the onset of shear-thickening and are shown in Figure 3. Shear-thickening behavior has been well-reviewed by Barnes (1989), where he observes "so many kinds of suspensions show shear-thickening that one is soon forced to the conclusion that given the right circumstances, all suspensions of solid particles will show the phenomenon."

Computer simulations of suspension dynamics allow the direct computation of the stress on each particle, and an ensemble average provides the total stress for the system. One can then perform simulation "experiments," which provide the detailed rheology and microstructure of the suspension. For example, Foss & Brady (2000) provide simulation results for suspensions in an infinite shear field for a wide range of Peclet numbers. They find the same shear-thinning and shear-thickening as observed in laboratory experiments.

Assuming a low shear rate Newtonian limit is also uncertain due to reports of yield stress behavior for some suspensions (Dabak & Yucel 1987, Heymann

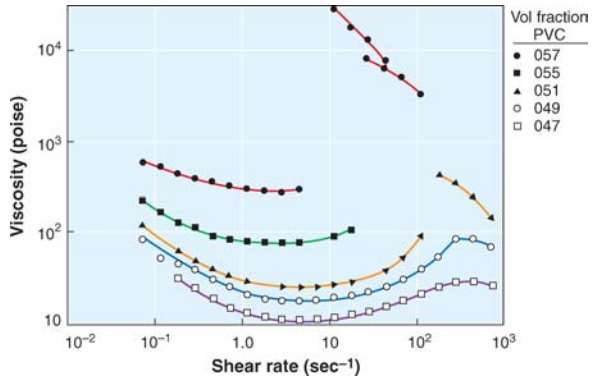

Figure 3 1.25 μm PVC particles in dioctyl phthalate (Hoffman 1972).

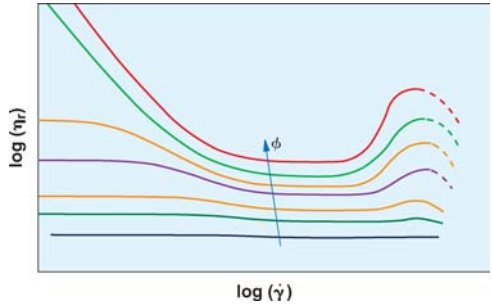

Figure 4 Representation of relative viscosity versus shear rate for a fluid suspension.

et al. 2002, Hoffman 1992, Jomha et al. 1991, Nguyen & Boger 1983, Zhu & De Kee 2002). The concept of a yield stress and its experimental measurement have been the subject of much debate (Barnes 1999, Heymann et al. 2002, Nguyen & Boger 1992). Nonetheless, an apparent yield stress has been clearly observed in suspensions, as indicated by a finite shear stress without deformation over long experimental time scales, or equivalently by a viscosity that tends toward infinity at vanishingly small shear rates. Yield stresses have mostly been detected at very high concentrations ($\phi > 0.5$). Some authors associate yield stress behavior with a solid-liquid phase transition of the suspensions (Heymann et al. 2002, Jomha et al. 1991).

We can now draw a qualitative picture of the non-Newtonian viscosity versus shear rate curve, as shown in Figure 4. In the zero shear rate limit, the suspension is Newtonian except for the yield stress behavior of very dense suspensions. All suspensions generally shear-thin at low to intermediate shear rates. With increasing shear rate, there is a Newtonian plateau and finally a steep shear-thickening region. The behavior beyond the shear-thickening region is not clear, but some studies indicate resumed shear-thinning if fracture does not occur first (Barnes 1989, Hoffman 1972).

To gain further insight into the non-Newtonian rheology of suspensions, it is useful to consider suspension microstructure. For suspensions of spherical particles, the microstructure is defined by the positions of the suspended particles relative to each other. Many different types of configurations are possible, e.g., strings, sheets, clumps, and semicrystalline groups; we provide analytical descriptions in section 4. It is now generally accepted that the non-Newtonian behavior of dense suspensions results from changes in microstructure under shear.

Völtz et al. (2002) photographed the outer surface of a suspension undergoing shearing flow between rotating concentric cylinders. They observed that an initially random suspension under shear became a two-dimensional hexagonal structure. This result supports the work of Hoffman (1972) in which he obtained light diffraction patterns for suspensions undergoing shear. From these diffraction

patterns he deduced that at low to moderate shear rates, for which the rheology was shear-thinning, the particles arranged into hexagonal packed sheets that slid over one another. At higher shear rates, with the onset of shear-thickening, the diffraction patterns did not indicate any organized structure. Unfortunately, Völtz et al. (2002) do not report shear-thickening results.

Based on the dimensional analysis of section 2, it seems reasonable to conclude that suspensions are shear-thinning when $\mathrm{Pe}_{\dot{\gamma}}$ is significant, shear-thickening when $\mathrm{Re}_{\dot{\gamma}}$ dominates, and Newtonian for a region where both can be neglected (Figure 1). This is supported by the microstructure results, which indicate ordered structure at low shear rate and disordered structure at high shear rate. However, Hoffman's (1972) suspensions begin to show shear-thickening behavior while still in the Peclet-dominated regime ($\mathrm{Pe}_{\dot{\gamma}} = 2 \times 10^2$, $\mathrm{Re}_{\dot{\gamma}} = 5 \times 10^{-8}$), although the suspensions of Völtz et al. (2002), which were shear-thinning for all of the shear rates tested, were in a region where finite Reynolds numbers are important ($\mathrm{Pe}_{\dot{\gamma}} = 8 \times 10^7$, $\mathrm{Re}_{\dot{\gamma}} = 1 \times 10^{-2}$). Clearly, neither the Peclet number nor the Reynolds number fully determine suspension rheology. Suspension microstructure dictates the rheology, and we must consider all factors that influence microstructure. While structure will certainly be a function of $\mathrm{Pe}_{\dot{\gamma}}$ and $\mathrm{Re}_{\dot{\gamma}}$, particle polydispersity, particle roughness, electrostatic, and van der Waals forces are also important. Although there are often attempts to minimize these nonhydrodynamic factors in laboratory experiments, their presence, no matter how small, can greatly affect the microstructure (Brady & Morris 1997).

Numerous authors have generated plots of relative suspension viscosity versus solids volume concentration in an attempt to correlate the two. In many early studies, neither the shear rates employed nor the particle polydispersity were carefully considered. Hence, the scatter in these correlations is quite severe (Rutgers 1962). Some investigators performed experiments exclusively in what they considered the low shear rate Newtonian limit (Chong et al. 1971, Krieger 1972, Storms et al. 1990) or alternatively in the high shear rate Newtonian limit (Chang & Powell 2002, Probstein et al. 1994).

Intuitively, the relative viscosity of a suspension will approach infinity as the volume fraction (ϕ) approaches some maximum value (ϕ_m):

$$\lim_{\phi \to \phi_m} \eta_r = \infty. \tag{7}$$

Physically, ϕ_m equates to the maximum packing fraction possible for a given suspension composition and packing arrangement. However, ϕ_m is often used as an adjustable parameter in viscosity models of the form

$$\eta_r = f\left(\frac{\phi}{\phi_m}\right). \tag{8}$$

In this sense, it is simply a direct scalar measure of suspension microstructure. The maximum packing fraction was not included in the dimensional analysis of section 2 because it is not an independent system variable. It depends on all the

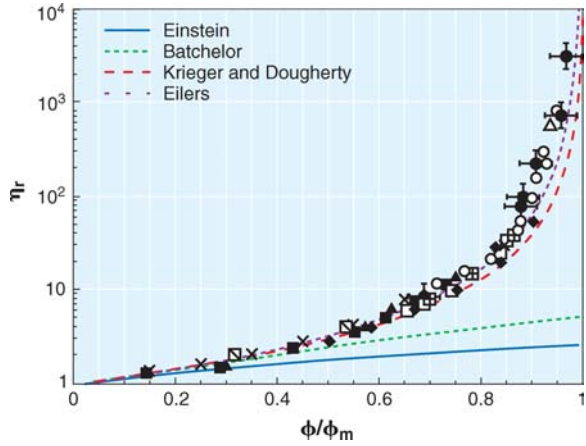

Figure 5 Relative viscosity as a function of reduced volume fraction. The line graphs correspond to models presented in the text, with $\phi_m = 0.65$ and $[\eta] = 2.5$. The symbols correspond to data presented in Chang & Powell (Chang & Powell 1994a).

parameters mentioned above that affect the microstructure of suspensions. By plotting η_r versus ϕ/ϕ_m and using appropriate values for ϕ_m, viscosity versus concentration plots collapse onto one curve (Figure 5) (Chang & Powell 1994a, Chang & Powell 2002, Chong et al. 1971, Wildemuth & Williams 1984).

When modeling the viscosity versus concentration relationship for suspensions, one must consider non-Newtonian behavior. One possible approach is to restrict ourselves to the high (or low) shear rate Newtonian regions, as depicted in Figure 4. The alternative is to include a shear rate–dependent term in the model, as discussed below. For a Newtonian fluid containing a dilute suspension of monodisperse particles ($\phi \to 0$), Einstein (1956) showed:

$$\eta_r = 1 + [\eta]\phi + O(\phi^2), \tag{9}$$

where $[\eta] = \frac{5}{2}$ for hard spheres. Batchelor (1977) and Batchelor & Green (1972) extended this relationship to second order:

$$\eta_r = 1 + [\eta]\phi + B\phi^2 + O(\phi^3), \tag{10}$$

where $B = 6.2$ for Brownian suspensions in any flow, and $B = 7.6$ for non-Brownian suspensions in pure straining flow.

For general models of relative viscosity versus particle concentration, it is worthwhile to consider how the model behaves in the limits of both high and low concentration. The limit of high concentration is given as Equation 7. At small ϕ, a relative viscosity function should take on the form of Equation 9:

$$\lim_{\phi \to 0} \frac{\eta_r - 1}{\phi} = [\eta]. \tag{11}$$

One empirical formula that obeys both the high and low concentration limits was given by Eilers (Ferrini et al. 1979):

$$\eta_r = \left(1 + \frac{\frac{1}{2}[\eta]\phi}{1 - \phi/\phi_m}\right)^2. \tag{12}$$

Another satisfactory model was derived by Krieger and Dougherty (1959). They considered the viscosity increase due to adding particles to a suspension already containing particles and obtained:

$$\eta_r = \left(1 - \frac{\phi}{\phi_m}\right)^{-[\eta]\phi_m}. \tag{13}$$

The form of Equation 13 can also be credited to Maron & Pierce (1956), although their exponent is given as -2 and hence does not explicitly satisfy Equation 11. Many other functions have been proposed and provide excellent fits to experimental data (Chong et al. 1971, Frankel & Acrivos 1967, Mooney 1951, Sengun & Probstein 1989). Characteristic plots of the viscosity versus concentration functions presented here are overlaid on experimental data in Figure 5.

The a priori prediction of the maximum packing fraction, ϕ_m, for a system of particles is still an open question, despite much study. By considering different geometric arrangements of monomodal spheres, a range of theoretical values for ϕ_m can be obtained, from the simple cubic value of 0.524 to the hexagonal close-packed value of 0.740 (Torquato et al. 2000). A well-mixed suspension does not self-assemble into one of the theoretical arrangements but instead forms a so-called random close-packed (RCP) arrangement. Settling experiments were used to find $\phi_m \approx 0.63$ for RCP (McGeary 1961).

For multimodal systems, it is more difficult to arrive at a theoretical value of ϕ_m. Qualitatively, small spheres may fit into the spaces between packed large spheres. Experiments of bimodal systems bear this out: ϕ_m increases with size ratio up to about 10:1, at which point the small spheres can completely fit into the empty spaces of the packed large spheres (McGeary 1961). The volume fraction ratio between large and small spheres is also important, with maximum packing obtained at about 60%–75% large particles (McGeary 1961, Shapiro & Probstein 1992). Trimodal, multimodal, and polydisperse systems can obtain even higher packing fractions. Models of packing fraction versus particle size distribution have been developed but are not reproduced here (Ouchiyama & Tanaka 1981, Zou et al. 2003).

Rheological experiments with bimodal, multimodal, and polydisperse systems emphasize the relation between ϕ_m and suspension viscosity. As expected, at equal total particle volume fraction the viscosities of multimodal systems are correspondingly lower than for their monodisperse counterparts, as Figure 6 shows (Chang & Powell 1994a, Chang & Powell 1994b, Chong et al. 1971).

Wildemuth & Williams (1984) propose an explicit flow dependence for ϕ_m. This is appealing because ϕ_m is a measure of microstructure, and microstructure changes with flow. Wildemuth & Williams (1984) derive a relationship where ϕ_m

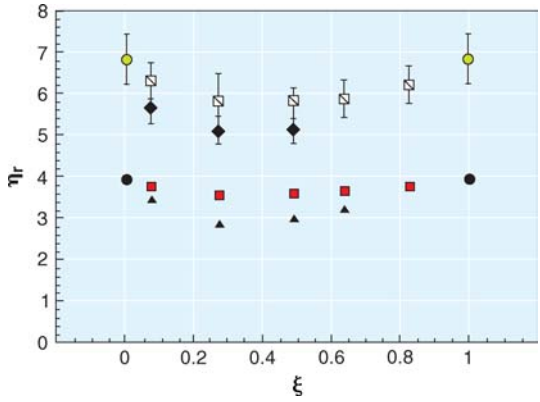

Figure 6 Relative viscosity versus fraction of small spheres, ξ, for fixed area fraction, $\phi_a = 0.6$, resulting from two-dimensional simulations (Chang & Powell 1994b). The symbols correspond to different size ratios and different simulation techniques.

is a function of shear stress and monotonically increases from ϕ_{m_0} at $\tau = 0$ to ϕ_{m_∞} as $\tau \to \infty$:

$$\phi_m = \left[\frac{1}{\phi_{m_0}} - \left(\frac{1}{\phi_{m_0}} - \frac{1}{\phi_{m_\infty}}\right)\left(\frac{1}{1 + A\tau^{-m}}\right)\right]^{-1}. \tag{14}$$

When substituted into an appropriate η_r versus ϕ/ϕ_m relationship, the result is a model that gives viscosity as a function of particle concentration and shear rate. As given, their equation for $\phi_m(\tau)$ predicts shear-thinning behavior and a yield stress. If a suspension had a concentration, say ϕ_1, which was greater than ϕ_{m_0} (but lower than ϕ_{m_∞}), it would not deform unless it were experiencing a shear stress greater than that required for $\phi_m(\tau)$ to equal ϕ_1. This stress is the yield stress, and it is clearly a function of concentration.

Another form for the relationship between suspension viscosity and shear rate is due to Krieger & Dougherty (1959) and Cross (1970):

$$\eta_r = \eta_\infty + \frac{\eta_0 - \eta_\infty}{1 + aD^n}, \tag{15}$$

where $D = \tau$ for Krieger and Dougherty (1959), and $D = \dot{\gamma}$ for Cross (1970). This model can generally be used to fit a shear-thinning viscosity. Cross (1970) also proposed a modified form for shear-thickening suspensions. Volume fraction dependency can be incorporated by letting $\eta_\infty = \eta_\infty(\phi)$ and $\eta_0 = \eta_0(\phi)$ in the form of Equation 13 (Krieger 1972).

Changes in suspension microstructure with flow are not instantaneous and give rise to time-dependent suspension rheology. Thixotropic behavior is common when a suspension thins with shear (Chang & Powell 1994a, Gadala-Maria & Acrivos 1980, Narumi et al. 2002, Voltz et al. 2002), and rheopectic behavior is common when a suspension shear-thickens (Barnes 1989, Hoffman 1974).

4. SUSPENSION MECHANICS

The shear viscosity of a suspension only partly characterizes its rheology. The entire stress tensor must be considered. This can be decomposed into the sum of three parts:

$$\mathbf{\Pi} = -p_o\mathbf{I} + 2\eta_o\dot{\boldsymbol{\gamma}} + \mathbf{\Pi}_p. \tag{16}$$

For the suspension systems considered here, p_o is the isotropic suspending fluid pressure, η_o is the viscosity of the Newtonian suspending fluid, and $\mathbf{\Pi}_p$ is the stress contribution from the suspended particles. We generally limit our discussion to simple shear flow. The rheology of suspensions in other types of flow, e.g., extensional flow, has not been well studied but is mentioned briefly elsewhere (Barnes 1989). For shear flow, the diagonal elements of $\dot{\boldsymbol{\gamma}}$ are identically zero, and the normal stress differences of the total stress tensor are given as: $N_1 := \Pi_{11} - \Pi_{22} = \Pi_{p,11} - \Pi_{p,22}$ and $N_2 := \Pi_{22} - \Pi_{33} = \Pi_{p,22} - \Pi_{p,33}$, where the flow, velocity gradient, and vorticity are in the 1, 2, and 3 coordinate directions, respectively. A particle phase isotropic pressure is also of interest, and is defined as $p_p := -\frac{1}{3}\mathrm{tr}(\mathbf{\Pi}_p)$. This pressure arises from the osmotic pressure induced by the particles, inter-particle forces, and flow-induced hydrodynamic normal stresses. The total isotropic pressure is then $p = p_o + p_p$.

It is well known that polymer solutions give rise to a positive N_1 and a smaller, negative N_2 (Tanner 1992). Normal-stress differences for suspensions are difficult to measure experimentally. Recently, Zarraga et al. (2000) performed a comprehensive study of suspension normal stresses using three different experimental techniques. For their non-Brownian suspensions, they show that both N_1 and N_2 are negative and proportional to shear stress, with $|N_2| > |N_1|$. In addition, they report that the flow induces a positive particle phase pressure.

Foss & Brady's (2000) simulation of an unbounded suspension undergoing shear flow also shows that N_2 is negative for all Peclet numbers simulated. However, N_1 is positive for low $\mathrm{Pe}_{\dot{\gamma}}$ and negative for high $\mathrm{Pe}_{\dot{\gamma}}$, crossing zero at $\mathrm{Pe}_{\dot{\gamma}} \sim O(1)$ (Figure 7). Singh & Nott (2000) performed dynamic simulations of a monolayer of non-Brownian suspended particles undergoing shear between semi-infinite plates. The resulting viscosity and first normal stress difference agree well with those of Zarraga et al. (2000) and Foss & Brady (2000) (for high $\mathrm{Pe}_{\dot{\gamma}}$).

Non-Newtonian stresses are generally caused by the microstructure. For fluids containing rods or polymers, normal stress differences arise from flow-alignment and/or stretching (Tucker & Moldenaers 2002). But hard spheres neither deform nor have a preferred direction. Instead, suspension microstructure is entirely dictated by the spatial arrangement of the particles, as discussed in section 3. Therefore, normal stress differences for suspensions arise from particle arrangements that have preferred directions. The microstructure of suspensions of hard spheres can be described by the pair-distribution function, $g(\mathbf{r})$. It describes the probability of finding a particle at position $\mathbf{r}$ relative to a reference particle, normalized by the number concentration of the suspension (Morris & Katyal 2002). Well-mixed

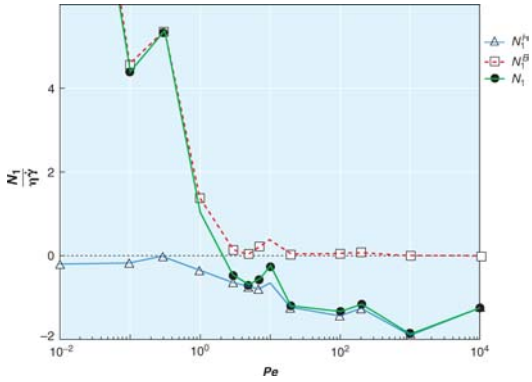

Figure 7 First normal stress difference for Stokesian dynamics simulation of 27 particles at $\phi = 0.45$ (Foss & Brady 2000).

suspensions with no flow history are generally isotropic, for which the pair distribution function only has a radial dependency caused by size exclusion. When a suspension undergoes flow, the particles may arrange to form an anisotropic configuration where there is a higher probability of finding particles in some directions than others, giving rise to an angular dependency.

The pair-distribution function can be determined from experiment if the position of each particle is known. However, large numbers of particles or long run times are needed for statistically significant results. Parsi & Gadala-Maria (1987) and Rampall et al. (1997) photographed suspensions undergoing shear and constructed the pair-distribution function in the shear plane. Fore-aft asymmetry was observed, but few other conclusions could be drawn from the data. The observed fore-aft asymmetry in $g(\mathbf{r})$ indicates that particle pairs spend more time in their approach than in their departure from one another. Suspension microstructure, including anisotropy, can also be measured by light-scattering and small-angle neutron-scattering experiments (Maranzano & Wagner 2002, Wagner & Russel 1990). Data from these experiments can be related to the pair-distribution function through a Fourier transform (Wagner & Ackerson 1992).

Computer simulations are particularly useful for understanding the dynamics of microstructure and its connection to rheology. As part of the computations, the positions of all the particles are exactly known at each time step. By averaging over many time steps, the full three-dimensional pair-distribution function can be obtained (Foss & Brady 2000, Morris & Katyal 2002, Sierou & Brady 2002). For a particular set of simulation conditions, Figure 8*a* shows the pair-distribution function projected onto the flow gradient (1,2 or x,y) plane. The size exclusion radial dependency is clearly observed by the definite shells of higher probability. Of the two inner shells shown in the plot, note the buildup of particle pairs on the compressional axis and depletion on the extensional axis. In a study of varying

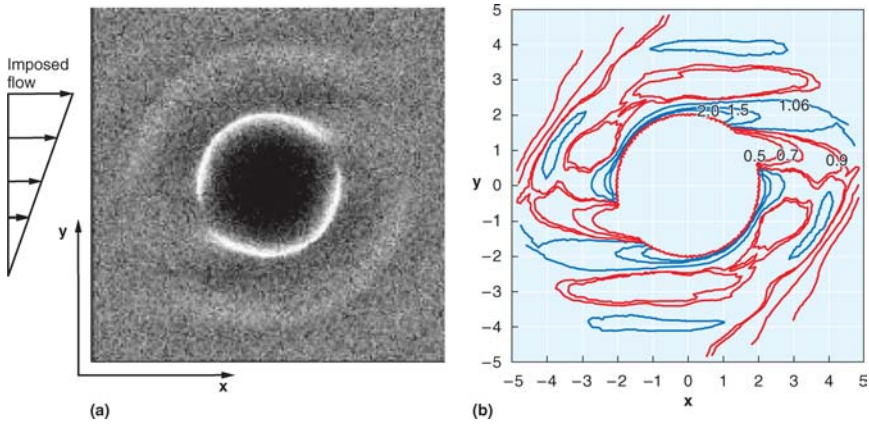

Figure 8 (*a*) Pair-distribution function projected onto the flow gradient plane for $\phi = 0.4$ (Sierou & Brady 2002). Lighter gray corresponds to higher probability. (*b*) Contour plot of $g(\mathbf{r})$ in the flow gradient plane for $\phi = 0.3$ and $\mathrm{Pe}_{\dot\gamma} = 25$ (Morris & Katyal 2002).

Peclet number, Morris & Katyal (2002) found that at elevated $\mathrm{Pe}_{\dot\gamma}$, $g(\mathbf{r})$ distorts to that illustrated in Figure 8*b*.

Batchelor (1977) and Batchelor & Green (1972) developed the first theoretical treatment of suspension fluid mechanics beyond the dilute limit. They demonstrated the explicit use of particle configuration probability, or the pair-distribution function, in determining the particle phase stress. Exact solutions for suspension viscosity were presented for semidilute suspensions in specific types of flow. Others proceeded to determine the normal stress differences and particle pressure as they first appear in dilute suspensions (Brady & Vicic 1995).

Determining $g(\mathbf{r})$ for nondilute suspensions in arbitrary flow fields is quite difficult. To our knowledge, only gross approximations and scaling analyses have been reported. In the asymptotic limit $\phi \to \phi_m$ for $\mathrm{Pe}_{\dot\gamma} \ll 1$, the stress is dominated by the Brownian contact stress:

$$\mathbf{\Pi}_p^{B1} = -4n^2kTa^3g_0(2a)\oint \hat{\mathbf{r}}\hat{\mathbf{r}}\,f(\mathbf{r})\,\mathrm{d}\mathbf{\Omega}, \tag{17}$$

where $\hat{\mathbf{r}}$ is the unit vector in direction $\mathbf{r}$, $g_0(r)$ is the pair distribution function at equilibrium, and $f(\mathbf{r}) := g(\mathbf{r})/g_0(r) - 1$ (Brady 1993, Brady & Vicic 1995). By evaluating perturbations of $f(\mathbf{r})$ with flow, an approximation for the components of $\mathbf{\Pi}_p$ can be determined to first order in Peclet number:

$$\eta_r \sim 1.3\beta^{-2} + O(\overline{\mathrm{Pe}}^2), \tag{18}$$

$$\frac{N_1}{\eta\dot\gamma} \sim 0.51\beta^{-2}\overline{\mathrm{Pe}} + O(\overline{\mathrm{Pe}}^2), \tag{19}$$

$$\frac{N_2}{\eta\dot\gamma} \sim -0.36\beta^{-2}\overline{\mathrm{Pe}} + O(\overline{\mathrm{Pe}}^2), \tag{20}$$

and

$$\frac{p_p}{nkT} \sim 2.9\beta^{-1} + 0.27\beta^{-1}\overline{\mathrm{Pe}}^2 + O(\overline{\mathrm{Pe}}^{5/2}), \tag{21}$$

where $\beta := (1 - \frac{\phi}{\phi_m})$ (Brady & Vicic 1995). $\overline{\mathrm{Pe}} = \frac{\dot{\gamma} a^2}{D_0^s(\phi)}$ is a Peclet number that scales with the concentration dependent short-time self-diffusivity, $D_0^s(\phi)$. This analytical result agrees with the simulation work of Foss & Brady (2000).

Brady & Morris (1997) show that the limit $\mathrm{Pe}_{\dot{\gamma}} \to \infty$ is singular and that any amount of Brownian motion, surface roughness, or nonhydrodynamic repulsion results in an asymmetric $g(\mathbf{r})$ and non-Newtonian stresses. They do not give an analytical result for $g(\mathbf{r})$ at high particle concentrations, but present a scaling analysis for $g(\mathbf{r})$ in a boundary layer about $g(2a)$ and comment on the possible values for the normal stress differences, specifically: $N_1 \approx 0$, and $N_2 < 0$.

Alternatively, terms that approximate the microstructure can be used for analysis and forming constitutive equations. Phan-Thien (1995) and Phan-Thien et al. (1999) considered concentrated suspensions to be composed of doublets of neighboring particles. With the unit vector connecting two particles in a doublet given by $\hat{\mathbf{r}}$, the structure tensors $\mathbf{Y}_2 := \langle \hat{\mathbf{r}}\hat{\mathbf{r}} \rangle$ and $\mathbf{Y}_4 := \langle \hat{\mathbf{r}}\hat{\mathbf{r}}\hat{\mathbf{r}}\hat{\mathbf{r}} \rangle$ can be defined. Their theoretical development results in a constitutive equation for the particle phase pressure:

$$\mathbf{\Pi}_p = \eta(\phi)[(1 - \xi)\dot{\boldsymbol{\gamma}} : \mathbf{Y}_4 + \dot{\gamma}(\mathbf{K} \cdot \mathbf{Y}_2 + \mathbf{Y}_2 \cdot \mathbf{K} + \mathrm{tr}(\mathbf{K})\mathbf{Y}_2 - 2\mathbf{K} : \mathbf{Y}_4)]. \tag{22}$$

ξ is a scalar value that depends on the separation distance of the sphere pair, and for touching spheres $\xi = 0.63$. Modeling of transient flows requires evolution equations for $\mathbf{Y}_2$ and $\mathbf{Y}_4$, which are also provided. The term $\mathbf{K}$, a dimensionless tensor that is a measure of anisotropy in particle self-diffusion (see section 5), was left partially undetermined by the authors. Phan-Thien et al. (2000) propose a phenomenological model for $\mathbf{K}$:

$$\mathbf{K} = K_3\mathbf{I} + (K_1 - K_3)\frac{2\mathbf{A}^{(1)} \cdot \mathbf{A}^{(1)}}{\mathrm{tr}(\mathbf{A}^{(1)} \cdot \mathbf{A}^{(1)})} + (K_2 - K_1)\frac{\mathbf{A}^{(2)} \cdot \mathbf{A}^{(2)}}{\mathrm{tr}(\mathbf{A}^{(2)} \cdot \mathbf{A}^{(2)})}, \tag{23}$$

where $\mathbf{A}^{(1)} = 2\dot{\boldsymbol{\gamma}}$ and $\mathbf{A}^{(2)} = \frac{\mathrm{D}}{\mathrm{D}t}\mathbf{A}^{(1)} + \boldsymbol{\nabla}\mathbf{v} \cdot \mathbf{A}^{(1)} + \mathbf{A}^{(1)} \cdot (\boldsymbol{\nabla}\mathbf{v})^T$ are the first two Rivlin-Ericksen tensors. K_i, $i = 1, 2, 3$, are constants that have certain restrictions for $\mathbf{K}$ to be positive semidefinite. Even so, different sets of K_i greatly influence the computed normal stress differences, including their sign (Phan-Thien et al. 2000). The model has proven quite good, at least qualitatively (Narumi et al. 2002, Phan-Thien et al. 2000).

5. SHEAR-INDUCED PARTICLE DIFFUSION

Shear-induced self-diffusion and particle migration in suspension flow has received considerable interest, starting principally with the work of Leighton & Acrivos (1987). They performed experiments that showed a diffusion-like process in which

particles migrate from regions of high shear rate to regions of low shear rate, even though their systems were non-Brownian and noninertial. It is well known that the trajectories of two isolated, interacting spheres undergoing Stokes' flow are symmetric and reversible. However, the simultaneous interactions of three or more spheres can lead to asymmetric net displacements that are irreversible (Breedveld et al. 2002, Drazer et al. 2002).

In a more general argument, Mauri (2003) refers to the Loschmidt paradox where microscopic reversible motion results in irreversible macroscopic phenomena. The paradox is resolved when one accounts for any small uncertainty or loss of information in the scaling from microscopic to macroscopic dynamics. In support of these arguments, Drazer et al. (2002) used simulations to explicitly measure the chaotic nature of suspension flow.

Although self-diffusion and bulk particle migration have the same origin, they have mostly been treated separately. Self-diffusion refers to the stochastic drift of tracer particles in uniform flow fields. Both computer simulations and physical experiments have shown that the average squared displacement of particles, minus the bulk flow displacement, grows linearly with dimensionless time, $\dot{\gamma}t$ (Breedveld et al. 2001, Marchioro & Acrivos 2001). Particle velocity fluctuations, v', have also been measured from which a "suspension temperature" can be defined: $T = \langle v'v' \rangle$ (Shapley et al. 2002). All together, these demonstrate a diffusion process, but on longer time scales than the Brownian motion. This self-diffusion is anisotropic, necessitating the use of a self-diffusion tensor (Breedveld et al. 2002, Foss & Brady 1999). Specifically, Breedveld et al. (2002) suggest:

$$\mathbf{D}^s_\infty = \dot{\gamma} a^2 \hat{\mathbf{D}}(\phi), \tag{24}$$

where $\hat{\mathbf{D}}(\phi)$ is a dimensionless symmetric tensor. The $\dot{\gamma}a^2$ scaling agrees with the theoretical treatment of Brady & Morris (1997). The ϕ dependence for the nonzero components of $\hat{\mathbf{D}}$ is less clear but is illustrated in Figure 9. The analysis of Brady & Morris (1997), where the development of microstructure is carefully considered, does predict $\hat{D}_{xx} > \hat{D}_{yy} > \hat{D}_{zz}$ and $\hat{D}_{xy} < 0$ (Foss & Brady 1999). However, all components of $\mathbf{D}^s_\infty$ are expected to increase with ϕ, which is not in agreement with the experimental results shown in Figure 9.

There is likely a direct connection between $\hat{\mathbf{D}}$ and the $\mathbf{K}$ of Equation 23. This has not yet been explored but could prove useful in constitutive models. It also illustrates a connection between the particle stress and shear-induced particle diffusion.

Shear-induced particle migration refers to the bulk migration of particles in nonuniform flows, as observed in many studies (Chow et al. 1994, Frank et al. 2003, Hampton et al. 1997, Nott & Brady 1994, Phan-Thien et al. 1995, Phillips et al. 1992). The net effect is inhomogeneous particle concentration, and therefore it is important in many practical applications. A few constitutive equations have been proposed to include particle migration. Based on the work of Leighton & Acrivos (1987), Phillips et al. (1992) developed a model that includes a particle flux term that is proportional to the shear gradient. This "diffusive flux"

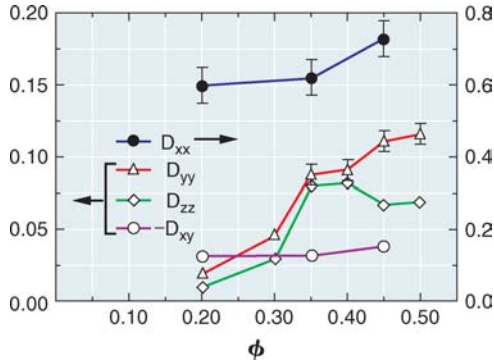

Figure 9 Concentration dependence for the nonzero components of $\hat{\mathbf{D}}$ (Breedveld et al. 2002). Note that $\hat{D}_{xy}$ is negative.

model provides satisfactory results for Couette & Poiseuille flow, but is inadequate for other viscometric flows, specifically the parallel plate and cone-and-plate geometries.

Another modeling approach employs mass and momentum balances over both the particle phase and the total suspension (Nott & Brady 1994). In this model the particle flux arises directly from the particle stress:

$$\mathbf{N}_p = h(\eta_s, a, \phi)\boldsymbol{\nabla} \cdot \boldsymbol{\Pi}_p, \tag{25}$$

where $h(\eta_s, a, \phi)$ is a hindered mobility coefficient (Fang et al. 2002, Morris & Boulay 1999). A constitutive equation for $\boldsymbol{\Pi}_p$ is required, for which Morris & Boulay (1999) and Fang et al. (2002) used simple approximations based on experimental data and scaling analyses (see section 4). Nonetheless, this "suspension balance" model provides excellent predictions of concentration and velocity profiles for several flow types (Figure 10) (Fang et al. 2002).

6. CONCLUDING REMARKS

Work over the last decade has provided significant insight into the mechanics of concentrated suspensions. Most efforts have focused on one particular aspect of suspension rheology, such as viscosity correlations, normal stress behavior, or particle migration. To obtain working models for use in flows of arbitrary geometry, all of these need to be considered together. Due to the complex and sometimes contradictory behavior reported in the literature, constitutive modeling of suspension fluid mechanics has been difficult. Nonetheless, considerable progress has been made by considering the suspension microstructure, which provides a physical rationale for the complex rheology of dense suspensions. Its inclusion has proved useful, even in simple semiempirical viscosity correlations where only a scalar description is necessary.

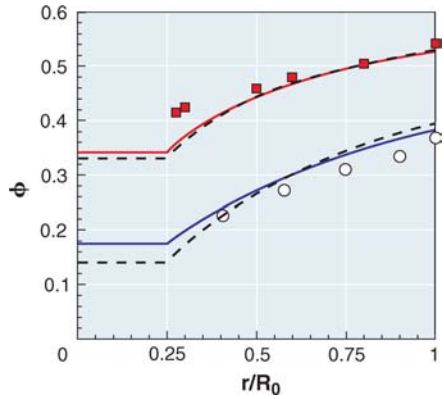

Figure 10 Suspension balance model prediction and experimental data for the truncated cone-and-plate geometry. Circles correspond to $\phi_b = 0.33$ and squares to $\phi_b = 0.50$ (ϕ_b = bulk volume concentration). Reprinted from Fang et al. (2002) with permission from Elsevier ©2002.

The full analytical treatment of suspension microstructure and its evolution with flow is quite complicated because the complete microstructure is given by the exact positions of all the particles. A more manageable description is required, with the most commonly used being the pair distribution function. Unfortunately, there has been only limited success in using the pair-distribution function in constitutive equations. Alternatively, Phan-Thien et al. (1999) used tensor descriptions of microstructure in forming a complete constitutive equation for particle stress with some success (Equation 22).

There has also been progress in the constitutive modeling of shear-induced particle migration. In particular, the suspension balance model gives accurate predictions for several flow geometries. This model demonstrates that particle migration arises from the particle stress (Equation 25), emphasizing the need for an adequate particle stress constitutive equation. Although microstructure does not appear explicitly in the suspension balance model, there is an implicit dependence due to the particle stress.

The above-mentioned constitutive equations were developed for monodisperse particle suspensions only. Although the shear viscosity of multimodal suspensions has been studied, there is no published work on the total particle stress and shear-induced diffusion of such systems. In addition, the prominent descriptions of microstructure, such as the pair distribution function, are not easily applied to multimodal suspensions. We do know how ϕ_m, an isotropic measure of microstructure, varies with polydispersity. A more complete description of suspension microstructure for multimodal systems needs to be developed that can then be used in constitutive models.

Lastly, a new generation of experiments that map both velocity and concentration fields in more complex flows would prove useful, e.g., flow in contraction and

expansion geometries. Some work has already been done with eccentric rotating cylinders (Phan-Thien et al. 1995), but data for suspensions in a wider range of non-viscometric flows are lacking. This will help in the development and verification of new constitutive models.

ACKNOWLEDGMENTS

The authors acknowledge Ronald Phillips for valuable discussions. This work was supported in part by the U.S. Department of Energy (DE-FG07-96R14727).

The *Annual Review of Fluid Mechanics* is online at http://fluid.annualreviews.org

LITERATURE CITED

Barnes HA. 1989. Shear-thickening (dilatancy) in suspensions of nonaggregating solid particles dispersed in Newtonian liquids. *J. Rheol.* 33(2):329–66

Barnes HA. 1999. The yield stress—a review or "παντα ρει"—everything flows? *J. Non-Newton. Fluid Mech.* 81(1–2):133–78

Barnes HA, Edwards MF, Woodcock LV. 1987. Applications of computer-simulations to dense suspension rheology. *Chem. Eng. Sci.* 42(4):591–608

Batchelor G. 1970. The stress system in a suspension of force-free particles. *J. Fluid Mech.* 41(3):545–70

Batchelor GK. 1977. Effect of Brownian-motion on bulk stress in a suspension of spherical-particles. *J. Fluid Mech.* 83(NOV): 97–117

Batchelor GK, Green JT. 1972. The determination of the bulk stress in a suspension of spherical particles to order c^2. *J. Fluid Mech.* 56(3):401–27

Boek ES, Coveney PV, Lekkerkerker HNW, van der Schoot P. 1997. Simulating the rheology of dense colloidal suspensions using dissipative particle dynamics. *Phys. Rev. E* 55(3):3124–33

Brady J. 1993. The rheological behavior of concentrated colloidal dispersions. *J. Chem. Phys.* 99(1):567–81

Brady JF, Bossis G. 1988. Stokesian dynamics. *Annu. Rev. Fluid Mech.* 20:111–57

Brady JF, Morris JF. 1997. Microstructure of strongly sheared suspensions and its impact on rheology and diffusion. *J. Fluid Mech.* 348:103–39

Brady JF, Vicic M. 1995. Normal stresses in colloidal dispersions. *J. Rheol.* 39(3):545–66

Breedveld V, van den Ende D, Bosscher M, Jongschaap RJJ, Mellema J. 2002. Measurement of the full shear-induced self-diffusion tensor of noncolloidal suspensions. *J. Chem. Phys.* 116(23):10529–35

Breedveld V, van den Ende D, Jongschaap R, Mellema J. 2001. Shear-induced diffusion and rheology of noncolloidal suspensions: Time scales and particle displacements. *J. Chem. Phys.* 114(13):5923–36

Chang CY, Powell RL. 1994a. Effect of particle-size distributions on the rheology of concentrated bimodal suspensions. *J. Rheol.* 38(1):85–98

Chang CY, Powell RL. 1994b. The rheology of bimodal hard-sphere dispersions. *Phys. Fluids* 6(5):1628–36

Chang CY, Powell RL. 2002. Hydrodynamic transport properties of concentrated suspensions. *AIChE J.* 48(11):2475–80

Chen S, Doolen GD. 1998. Lattice Boltzmann method for fluid flows. *Annu. Rev. Fluid Mech.* 30:329–64

Chong JS, Christiansen EB, Baer AD. 1971. Rheology of concentrated suspensions. *J. Appl. Polym. Sci.* 15:2007–21

Chow AW, Sinton SW, Iwamiya JH, Stephens TS. 1994. Shear-induced particle migration in Couette and parallel-plate viscometers—NMR imaging and stress measurements. *Phys. Fluids* 6(8):2561–76

Cross MM. 1970. Kinetic interpretation of non-Newtonian flow. *J. Colloid Interface Sci.* 33(1):30–35

Dabak T, Yucel O. 1987. Modeling of the concentration and particle-size distribution effects on the rheology of highly concentrated suspensions. *Powder Technol.* 52(3):193–206

Drazer G, Koplik J, Khusid B, Acrivos A. 2002. Deterministic and stochastic behaviour of non-Brownian spheres in sheared suspensions. *J. Fluid Mech.* 460:307–35

Einstein A. 1956. *Investigations on the Theory of the Brownian Movement*. New York: Dover

Fang ZW, Mammoli AA, Brady JF, Ingber MS, Mondy LA, Graham AL. 2002. Flow-aligned tensor models for suspension flows. *Int. J. Multiph. Flow* 28(1):137–66

Ferrini F, Ercolani D, Cindio BD, Nicodemo L, Nicolais L, Ranaudo S. 1979. Shear viscosity of settling suspensions. *Rheol. Acta* 18(2):289–96

Foss DR, Brady JF. 1999. Self-diffusion in sheared suspensions by dynamic simulation. *J. Fluid Mech.* 401:243–74

Foss DR, Brady JF. 2000. Structure, diffusion and rheology of Brownian suspensions by Stokesian Dynamics simulation. *J. Fluid Mech.* 407:167–200

Frank M, Anderson D, Weeks ER, Morris JF. 2003. Particle migration in pressure-driven flow of a Brownian suspension. *J. Fluid Mech.* 493:363–78

Frankel NA, Acrivos A. 1967. On the viscosity of a concentrated suspension of solid spheres. *Chem. Eng. Sci.* 22(6):847–53

Gadala-Maria F, Acrivos A. 1980. Shear-induced structure in a concentrated suspension of solid spheres. *J. Rheol.* 24(6):799–814

Glowinski R, Pan TW, Hesla TI, Joseph DD. 1999. A distributed Lagrange multiplier fictitious domain method for particulate flows. *Int. J. Multiph. Flow* 25(5):755–94

Hampton RE, Mammoli AA, Graham AL, Tetlow N, Altobelli SA. 1997. Migration of particles undergoing pressure-driven flow in a circular conduit. *J. Rheol.* 41(3):621–40

Heymann L, Peukert S, Aksel N. 2002. On the solid-liquid transition of concentrated suspensions in transient shear flow. *Rheol. Acta* 41(4):307–15

Hill RJ, Koch DL, Ladd AJC. 2001. The first effects of fluid inertia on flows in ordered and random arrays of spheres. *J. Fluid Mech.* 448:213–41

Hoffman RL. 1972. Discontinuous and dilatant viscosity behavior in concentrated suspensions. I. Observation of a flow instability. *Trans. Soc. Rheol.* 16:155–73

Hoffman RL. 1974. Discontinuous and dilatant viscosity behaviour in concentrated suspensions. II. Theory and experimental tests. *J. Colloid Interface Sci.* 46:491–506

Hoffman RL. 1992. Factors affecting the viscosity of unimodal and multimodal colloidal dispersions. *J. Rheol.* 36(5):947–65

Hoogerbrugge PJ, Koelman JMVA. 1992. Simulating microscopic hydrodynamic phenomena with dissipative particle dynamics. *Europhys. Lett.* 19(3):155–60

Jomha AI, Merrington A, Woodcock LV, Barnes HA, Lips A. 1991. Recent developments in dense suspension rheology. *Powder Technol.* 65(1–3):343–70

Krieger IM. 1963. A dimensional approach to colloid rheology. *Trans. Rheol. Soc.* 7:101–9

Krieger IM. 1972. Rheology of monodisperse latices. *Adv. Colloid Interface Sci.* 3:111–36

Krieger IM, Dougherty TJ. 1959. A mechanism for non-Newtonian flow in suspensions of rigid spheres. *Trans. Soc. Rheol.* 3:137–52

Leighton D, Acrivos A. 1987. The shear-induced migration of particles in concentrated suspensions. *J. Fluid Mech.* 181:415–39

Maranzano BJ, Wagner NJ. 2002. Flow-small angle neutron scattering measurements of colloidal dispersion microstructure evolution

through the shear thickening transition. *J. Chem. Phys.* 117(22):10291–302

Marchioro M, Acrivos A. 2001. Shear-induced particle diffusivities from numerical simulations. *J. Fluid Mech.* 443:101–28

Maron SH, Pierce PE. 1956. Application of Ree-Eyring generalized flow theory to suspensions of spherical particles. *J. Colloid Sci.* 11:80–95

Mauri R. 2003. The constitutive relation of suspensions of noncolloidal particles in viscous fluids. *Phys. Fluids* 15(7):1888–96

McGeary RK. 1961. Mechanical packing of spherical particles. *J. Am. Ceram. Soc.* 44(10):513–22

Metzner AB, Whitlock M. 1958. Flow behavior of concentrated (dilatent) suspensions. *Trans. Soc. Rheol.* 2:239–54

Mooney M. 1951. The viscosity of a concentrated suspension of spherical particles. *J. Colloid Sci.* 6:162–70

Morris JF, Boulay F. 1999. Curvilinear flows of noncolloidal suspensions: The role of normal stresses. *J. Rheol.* 43(5):1213–37

Morris JF, Katyal B. 2002. Microstructure from simulated Brownian suspension flows at large shear rate. *Phys. Fluids* 14(6):1920–37

Narumi T, See H, Honma Y, Hasegawa T, Takahashi T, Phan-Thien N. 2002. Transient response of concentrated suspensions after shear reversal. *J. Rheol.* 46(1):295–305

Nguyen QD, Boger DV. 1983. Yield stress measurement for concentrated suspensions. *J. Rheol.* 27(4):321–49

Nguyen QD, Boger DV. 1992. Measuring the flow properties of yield stress fluids. *Annu. Rev. Fluid Mech.* 24:47–88

Nott PR, Brady JF. 1994. Pressure-driven flow of suspensions—simulation and theory. *J. Fluid Mech.* 275:157–99

Ouchiyama N, Tanaka T. 1981. Porosity of a mass of solid particles having a range of sizes. *Ind. Eng. Chem. Fundam.* 20(1):66–71

Parsi F, Gadala-Maria F. 1987. Fore-and-aft asymmetry in a concentrated suspension of solid spheres. *J. Rheol.* 31(8):725–32

Phan-Thien N. 1995. Constitutive equation for concentrated suspensions in newtonian liquids. *J. Rheol.* 39(4):679–95

Phan-Thien N, Fan XJ, Khoo BC. 1999. A new constitutive model for monodispersed suspensions of spheres at high concentrations. *Rheol. Acta* 38(4):297–304

Phan-Thien N, Fan XJ, Zheng R. 2000. A numerical simulation of suspension flow using a constitutive model based on anisotropic interparticle interactions. *Rheol. Acta* 39(2):122–30

Phan-Thien N, Graham AL, Altobelli SA, Abbott JR, Mondy LA. 1995. Hydrodynamic particle migration in a concentrated suspension undergoing flow between rotating eccentric cylinders. *Ind. Eng. Chem. Res.* 34(10):3187–94

Phillips RJ, Armstrong RC, Brown RA, Graham AL, Abbott JR. 1992. A constitutive equation for concentrated suspensions that accounts for shear-induced particle migration. *Phys. Fluids A* 4(1):30–40

Probstein RF, Sengun MZ, Tseng TC. 1994. Bimodal model of concentrated suspension viscosity for distributed particle sizes. *J. Rheol.* 38(4):811–29

Rampall I, Smart JR, Leighton DT. 1997. The influence of surface roughness on the particle-pair distribution function of dilute suspensions of non-colloidal spheres in simple shear flow. *J. Fluid Mech.* 339:1–24

Rutgers IR. 1962. Relative viscosity of suspensions of rigid spheres in Newtonian liquids. *Rheol. Acta* 2:202–10

Sato T. 1995. Rheology of suspensions. *J. Coat. Technol.* 67(847):69–79

Sengun MZ, Probstein RF. 1989. High-shear-limit viscosity and the maximum packing fraction in concentrated monomodal suspensions. *Physicochem. Hydrodyn.* 11(2):229–41

Shapiro AP, Probstein RF. 1992. Random packings of spheres and fluidity limits of monodisperse and bidisperse suspensions. *Phys. Rev. Lett.* 68(9):1422–25

Shapley NC, Armstrong RC, Brown RA. 2002. Laser Doppler velocimetry measurements of

particle velocity fluctuations in a concentrated suspension. *J. Rheol.* 46(1):241–72

Sierou A, Brady JF. 2001. Accelerated Stokesian Dynamics simulations. *J. Fluid Mech.* 448:115–46

Sierou A, Brady JF. 2002. Rheology and microstructure in concentrated noncolloidal suspensions. *J. Rheol.* 46(5):1031–56

Singh A, Nott PR. 2000. Normal stresses and microstructure in bounded sheared suspensions via Stokesian Dynamics simulations. *J. Fluid Mech.* 412:279–301

Singh P, Hesla TI, Joseph DD. 2003. Distributed Lagrange multiplier method for particulate flows with collisions. *Int. J. Multiph. Flow* 29(3):495–509

So JH, Yang SM, Hyun JC. 2001. Microstructure evolution and rheological responses of hard sphere suspensions. *Chem. Eng. Sci.* 56(9):2967–77

Storms RF, Ramarao BV, Weiland RH. 1990. Low shear rate viscosity of bimodally dispersed suspensions. *Powder Technol.* 63(3):247–59

Tanner RI. 1992. *Engineering Rheology*. The Oxford Eng. Sci. Ser. New York: Oxford Univ. Press. Rev. ed. 451 pp.

Torquato S, Truskett TM, Debenedetti PG. 2000. Is random close packing of spheres well defined? *Phys. Rev. Lett.* 84(10):2064–67

Tucker CL, Moldenaers P. 2002. Microstructural evolution in polymer blends. *Annu. Rev. Fluid Mech.* 34:177–210

Voltz C, Nitschke M, Heymann L, Rehberg I. 2002. Thixotropy in macroscopic suspensions of spheres. *Phys. Rev. E* 65(5):051402

Wagner NJ, Ackerson BJ. 1992. Analysis of nonequilibrium structures of shearing colloidal suspensions. *J. Chem. Phys.* 97(2): 1473–83

Wagner NJ, Russel WB. 1990. Light-scattering measurements of a hard-sphere suspension under shear. *Phys. Fluids A* 2(4):491–502

Wildemuth CR, Williams MC. 1984. Viscosity of suspensions modeled with a shear-dependent maximum packing fraction. *Rheol. Acta* 23(6):627–35

Zarraga IE, Hill DA, Leighton DT. 2000. The characterization of the total stress of concentrated suspensions of noncolloidal spheres in Newtonian fluids. *J. Rheol.* 44(2):185–220

Zhu LX, De Kee D. 2002. Slotted-plate device to measure the yield stress of suspensions: Finite element analysis. *Ind. Eng. Chem. Res.* 41(25):6375–82

Zou RP, Xu JQ, Feng CL, Yu AB, Johnston S, Standish N. 2003. Packing of multi-sized mixtures of wet coarse spheres. *Powder Technol.* 130(1–3):77–83

Annual Review of Fluid Mechanics
Volume 37, 2005

CONTENTS